Quasisteady MPD Arcjet with Hollow Cathode

K. Toki*
Institute of Space and Astronautical Science, Tokyo, Japan

Hollow cathodes with various diameters and interelectrode lengths were tested to evaluate their effects on the performance of a magnetoplasmadynamic (MPD) thruster. The thruster was operated in a quasisteady mode in the specific impulse (Isp) range of 1000-2000 s. The arc chamber was designed so that its wall formed a divergent nozzle and the hollow cathode constituted a part of the flow tube. The entire propellant was injected through the hollow cathode and forced to be heated in the arc column so as to enhance the aerodynamic acceleration. An appropriate combination of cathode interior diameter and interelectrode length resulted in the maximum thrust power ratio of 25 mN/kW for hydrogen and a lower cathode erosion rate than occurs with a solid cathode. However, a similar configuration was not effective for ammonia propellant because the mass flow was interrupted by excessively high pressure due to induced electromagnetic pinch force in the hollow cathode interior. Consequently, the hollow cathode exhibited inferior thrust performance but superior erosion characteristics compared to the solid cathode.

Introduction

HOLLOW cathodes have been widely used in ion thrusters because of their unique advantage of small electrode erosion rate, which reduces plasma contamination inside the hollow cathode and enhances the longevity of this critical component. In the 1960s it was found that the dc magnetoplasmadynamic (MPD) thruster with a hollow cathode exhibited better performance in terms of thermal efficiency and cathode lifetime than conventional solid cathode configurations.[1,2]

For these reasons, hollow cathodes were intensively investigated in the late 1970s, using the quasisteady MPD arcjet.[3,4] These efforts were focused mainly on understanding the physical processes occurring inside the hollow cathode, such as current and potential distribution, the ionization process, and electron emission mechanism. It was concluded that the current penetration about one diameter upstream into the cathode interior allows efficient ionization and heating of propellant passing through the hollow cathode. However, data are sparse concerning hollow cathodes applied to a high current MPD thruster operating in the quasisteady mode.[5]

In our experiment, hollow cathodes with various interior diameters and interelectrode lengths were fabricated to survey their thrust performance in the specific impulse (Isp) range of 1000-2000 s. In this Isp range, it is considered that the thrust-producing mechanism depends on electrothermal contribution as well as electromagnetic blowing contributions.[6] Therefore hollow cathodes are expected to be advantageous and suitable in the above Isp range. Since it has already been recognized that at high current operation (over several kA) most of the increased current does not penetrate inside the hollow cathode but flows to the outer barrel, a hollow cathode should be incorporated into the arc chamber without exposing the cathode exterior to the discharge. Such a configuration is realized when the hollow cathode forms a part of the flow tube in the arc chamber. Thus, the entire propellant can be injected through the arc column to be effectively ionized and heated before the nozzle expansion. The major objective of this experiment is to evaluate this concept and develop guidelines for improving hollow cathode MPD thruster performance.

Experimental Apparatus and Procedure

Figure 1 shows the baseline configuration of a hollow cathode MPD thruster in this experiment. According to the foregoing concept, the hollow cathode forms a part of the flow tube in a divergent nozzle with its exterior surface covered by an interelectrode insulator. The copper nozzle has a 60-mm exit diameter with 20-deg half-angle divergence. The boron-nitride interelectrode insulator has a 30-mm exit diameter with various divergence half-angles suitable for the corresponding hollow cathode to be tested. The cathodes are made of 2% thoriated tungsten. The thruster head is set in a stainless-steel vacuum tank of 1.5-m diam and 2.5-m length, which is evacuated less than 7 mPa before each firing.

Hydrogen and ammonia propellant is injected radially into the hollow cathode passage through eight ports located at the cathode circumference. One of these ports can be occupied by a pressure transducer monitoring upsteam pressure in the hollow passage during the operation. Propellant mass flow rates are regulated by both the reservoir pressure of fast-acting valves and their choke orifice diameters. The fast-acting valves operate at the maximum reservoir pressure of 5 atm and generate a 3-ms flat-topped gas pulse.

The electrical power source consists of a five-station pulse-forming network having 2000-μF capacitance at the maximum charging voltage of 4 kV. The current pulse has a width of 1 ms in rectangular form. The arc discharge is initiated by an ignition switch, which closes the discharge circuit after the propellant mass flow rate reaches a constant value. The discharge current was measured by a Rogowski coil with integrating circuit, and the voltage was obtained by a current probe sensing the small current through a high impedance shunt resistor connected between the anode and the cathode.

The thrust measurements were conducted by the parallelo-pendulum method. The thruster was suspended from the tank ceiling by two pairs of steel wires. The deflection of the parallelo-pendulum was detected by a linear transformer and was calibrated by known impulses. The impulse bit of cold gas that had been measured prior to thruster firing was subtracted from the fired impulse bit. The subtracted value can be transformed into thrust by dividing the quasisteady duration. Major error in the thrust measurement arose from shot-by-

Presented as Paper 85-2057 at the AIAA/DGLR/JSASS 18th International Electric Propulsion Conference, Alexandria, VA, Sept. 30-Oct. 2, 1985; received Dec. 20, 1985; revision received April 30, 1986.

*Research Associate. Member AIAA.

shot deviation; however, it was less than 5% of the averaged value of several shots. The thrust performance data were evaluated in terms of the following parameters:

$$\text{Isp} = T(\dot{m}g), \quad \eta = T^2/(2\dot{m}JV), \quad T_P = T/(JV)$$

Isp denotes specific impulse, T thrust, $\dot{m}$ propellant mass flow rate, g gravitational acceleration, η thrust efficiency, J discharge current, V discharge voltage, and T_p thrust power ratio. The electromagnetic blowing force F_b and pumping force F_p are expressed as follows:

$$F_b = (\mu_0 J^2/4\pi)\,[\ell n w + b(x,y)], \quad F_p = \mu_0 J^2/8\pi$$

$$w = R_{a\min}/R_{c\max}, \quad x = R_{a\max}/R_{a\min}, \quad y = R_{c\min}/R_{c\max}$$

where $R_{a_{max}}$ equals maximum anode radius, $R_{a_{min}}$ minimum anode radius, $R_{c_{max}}$ maximum cathode radius, and $R_{c_{min}}$ minimum cathode radius.

The blowing force F_b is deduced from integrating Lorentz force under the postulation of spatially uniform current distribution between the conical anode and the cathode. Here $b(x,y)$ is defined as the function of electrodes radius ratio.[7]

Table 1 lists the various cathode configurations that were used in this experiment. Hollow cathode diameters D of 16, 10, and 6 mm were used with a fixed 12-mm interelectrode length. Axial interelectrode length L equal to 12, 20, and 28 mm, were used in conjunction with the 10-mm hollow cathode diameter. As shown in Fig. 2, a recessed cathode was inserted at the center of the hollow cathode passage in both extreme cases, namely, the 6-mm cathode diameter and the 28-mm interelectrode length. Before these modifications, the thruster frequently misfired at low currents and high propellant mass flow rates. The recessed cathode design served to decrease the number of misfirings and, once the arc discharge was initiated, it did not affect thruster performance. Since the arc spot radius and column length at high current density are determined by the hollow cathode diameter and interelectrode length, respectively, the smaller hollow cathode diameter emphasizes the electromagnetic blowing force while the longer interelectrode length enhances the electrothermal heating component. Therefore, it is possible to use these parameters to qualitatively control the ratio between the electromagnetic and electrothermal contribution to measured thruster performance. In addition to the above hollow cathode studies, data were also obtained with a solid cathode for comparison. The solid cathode configuration is also shown in Fig. 2. This design configuration recorded the best thrust performance observed to date.[8]

For all these configurations, discharge currents and propellant mass flow rates were varied from 4.5 to 9.0 kA, from 0.6 to 1.2 g/s for hydrogen, and from 1.2 to 2.4 g/s for ammonia, respectively.

Table 1 Tested hollow cathode diameter D and interelectrode length L (X = variations)

		L, mm		
		12	20	28
D, mm	6	X		
	10	Baseline	X	X
	16	X		

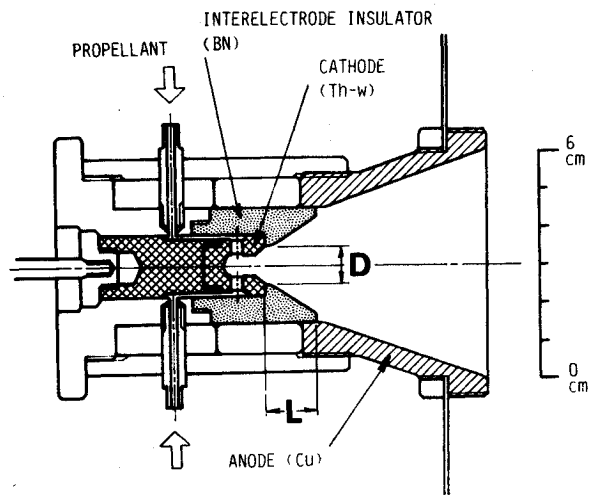

Fig. 1 Hollow cathode baseline configuration.

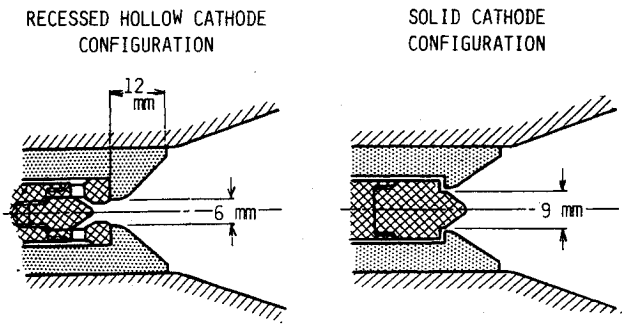

Fig. 2 Recessed hollow cathode configuration and solid cathode configuration.

Experimental Results and Discussion

Hollow Cathode Baseline Configuration

Figures 3 and 4 show the discharge voltage vs current and the thrust vs current data, respectively, for the hollow cathode baseline configuration: 10-mm (medium) hollow cathode diameter and 12-mm (short) interelectrode length. In Fig. 4, the solid line T_{em} represents the electromagnetic thrust produced by both blowing F_b and pumping F_p forces.

In general, ammonia propellant was characterized by lower discharge voltage and thrust than hydrogen propellant for all the mass flow rates. These tendencies are not peculiar to hollow cathodes but are also present during solid cathode operation. Another remarkable feature of ammonia propellant was revealed—that the discharge voltage is insensitive to propellant mass flow rate while that of hydrogen propellant increases with mass flow rates. This phenomenon would reflect the electron mobility against particle collisions in the arc chamber. Since ammonia has inherently lower ionization potential than hydrogen and also has lower number density in the arc chamber by one order of magnitude than that of hydrogen propellant at the same mass flow rate, ammonia should be regarded as fully ionized, with the electron mobility dominated by Coulomb collisions. Consequently, the discharge voltage of ammonia propellant would become insensitive to the above range of particle densities and the mass flow rates. Figure 3 shows this independence of the discharge voltage on mass flow rate for ammonia except at the low flow rate of 1.2 g/s, which showed higher voltages at higher current levels. Strong voltage fluctuation suggests that severe starvation occurred. Starvation corresponds to the retardation of mass flow inside the hollow cathode due to back electromagnetic force acting in the upstream direction. This will be discussed later. In Fig. 4, the measured thrust reveals strong dependence on the propellant mass flow rates for both propellants as is usual in the relatively low Isp range. These phenomena in the hollow cathode baseline configuration were commonly observed among other hollow cathode configurations.

Effects of Hollow Cathode Diameters

Figure 5 shows the discharge voltage vs current characteristics for various hollow cathode diameters at a mass flow rate of 1.8 g/s. In this figure, the voltages increase with decreasing hollow cathode diameter for both the hydrogen and ammonia propellants. The voltage increase brought about by changing hollow cathode diameter generally corresponds to the thrust increase, as shown in Fig. 6. This is true except for the 6-mm hollow cathode diameter data for ammonia where starvation occurred. This correlation between the increase of thrust and voltage implies that the back EMF caused by electromagnetic blowing acceleration is mainly responsible for the voltage increment. The increase in both thrust and voltage may explain why the measured thrust power ratio is insensitive to the change of hollow cathode diameter and lies at about 20 mN/kW in Fig. 7. Therefore, it should be concluded that further reduction of hollow cathode diameter will not improve thrust efficiency.

Figure 8 shows the hollow cathode pressure variation for different diameters. It is apparent that for both hydrogen and ammonia propellants the hollow cathode pressure has a much higher value than the prediction of electromagnetic pumping pressure Ph,p. The significantly different behavior of these two propellants can be attributed to their particle densities. The hydrogen pressure is slightly increased by decreasing hollow cathode diameter, while the ammonia pressure is drastically changed from 0.6 atm up to about 2 atm by decreasing hollow cathode diameter and increasing discharge current. While these high internal pressures are preferable for thrust production, the excessive rise in pressure acts as a back force on the propellant mass flow and consequently destroys the choked condition of the upstream fast-acting valves.

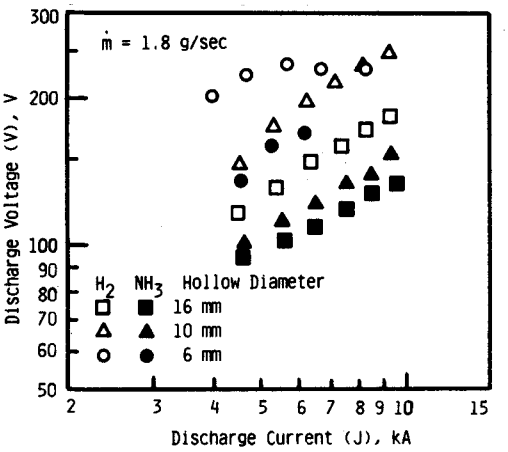

Fig. 5 Discharge voltage vs current characteristics for various hollow cathode diameters.

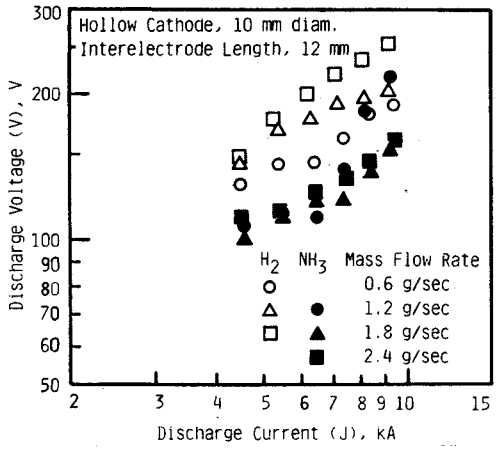

Fig. 3 Discharge voltage vs current characteristics for hollow cathode baseline configuration.

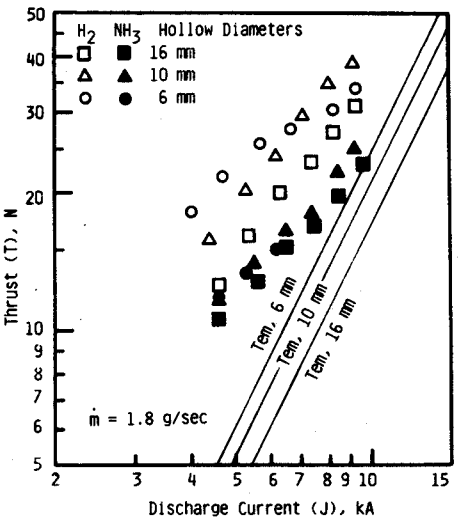

Fig. 6 Thrust vs current characteristics for various hollow cathode diameters.

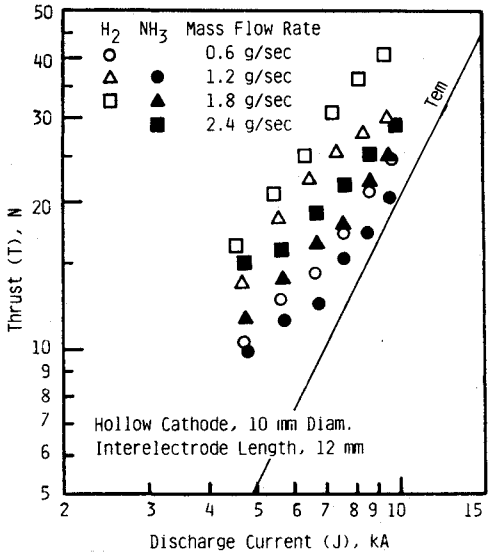

Fig. 4 Thrust vs current characteristics for hollow cathode baseline configuration.

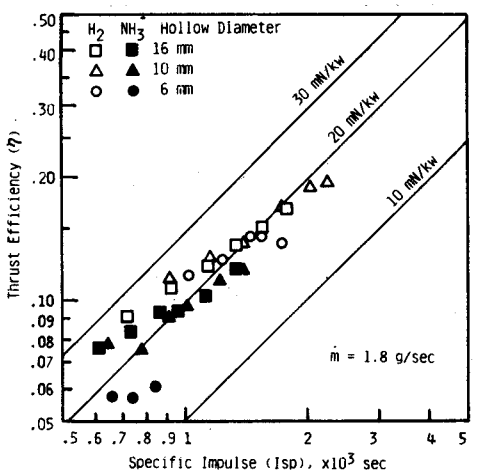

Fig. 7 Thrust efficiency vs Isp plot for various hollow cathode diameters.

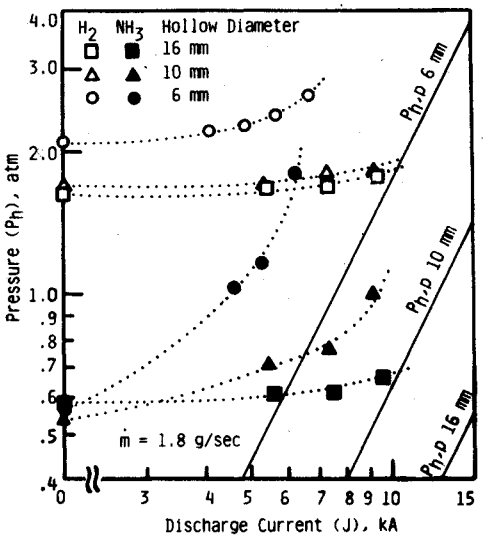

Fig. 8 Hollow cathode pressure variation for various hollow cathode diameters.

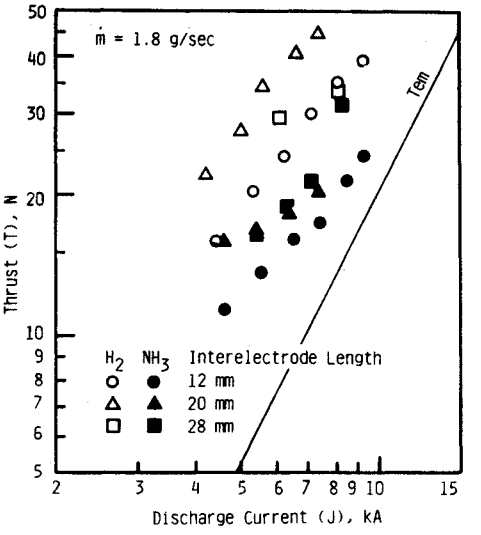

Fig. 10 Thrust vs current characteristics for various interelectrode lengths.

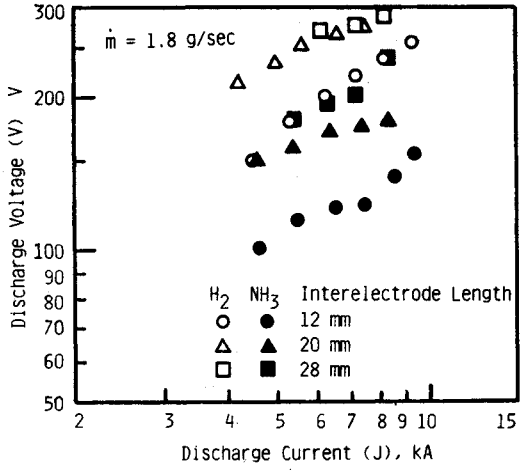

Fig. 9 Discharge voltage vs current characteristics for various interelectrode lengths.

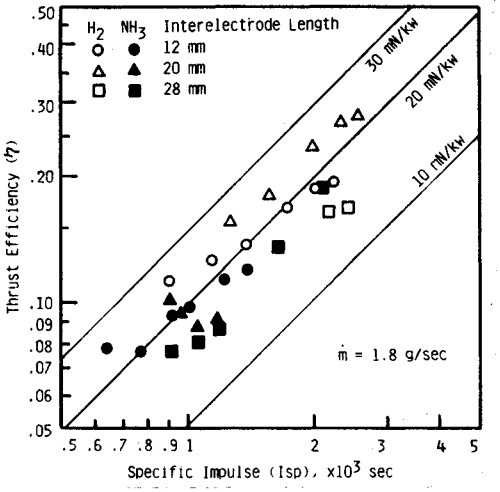

Fig. 11 Thrust efficiency vs Isp plot for various interelectrode lengths.

Figure 9 shows the effect of interelectrode length on the discharge voltage vs current characteristics at a propellant mass flow rate of 1.8 g/s.The voltage is increased, together with a drastic thrust increase, as shown in Fig. 10, by increasing interelectrode length from 12 mm (short) to 20 mm (medium) for both hydrogen and ammonia propellant. However, in the long case (28 mm) for hydrogen, the operation suffered from frequent delays of arc initiation and finally misfired at lower currents. It is also found that the voltage vs current characteristics become rather flat for longer interelectrode length, whereas the thrust vs current curves merely shift upward with increasing interelectrode length. These features are reasonable if the electrothermal heating of propellant is enhanced by an extended arc column. Although the elongated interelectrode length tends to increase the arc impedance, the arc current flows through the electrothermally pinched and highly ionized column so as to lower the arc voltage. This mechanism would make the discharge voltage insensitive to current and increase the electrothermal thrust produced by effective energy transfer from the elongated arc column to the propellant.

Figure 11 shows the obtained thrust efficiency vs Isp data for various interelectrode lengths. For hydrogen propellant, the thrust power ratio is as large as 25 mN/kW for the 20-mm medium interelectrode length, but further elongation of in-

Table 2 Cathode and insulator erosion, $\mu g/C$, for different hollow diameters

	D, mm	H_2	NH_3
Cathode	16	10.9	11.9
	10	4.5	5.1
	6	3.5 (11.1)[a]	1.4 (0)
Insulator	16	−4.0[b]	10.1
	10	9.4	4.7
	6	54.7	11.8

[a] ( ) = recessed cathode. [b] − = deposit.

Table 3 Cathode and insulator erosion, $\mu g/C$, for different interelectrode lengths

	L, mm	H_2	NH_3
Cathode	12	4.5	5.1
	20	3.2	1.9
	28	1.3 (2.2)[a]	−4.7 (−20.0)[b]
Insulator	12	9.4	4.7
	20	2.5	37.1
	28	17.3	76.3

[a] ( ) = recessed cathode. [b] − = deposit.

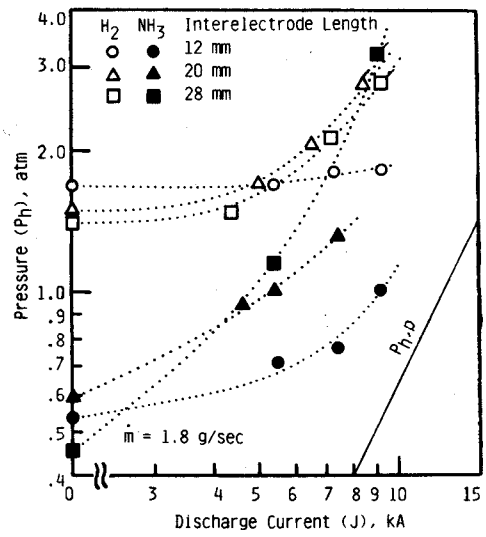

Fig. 12 Variation of hollow cathode pressure for various interelectrode lengths (for dashed data points, $\dot{m}$ was not exactly regulated at 1.8 g/s).

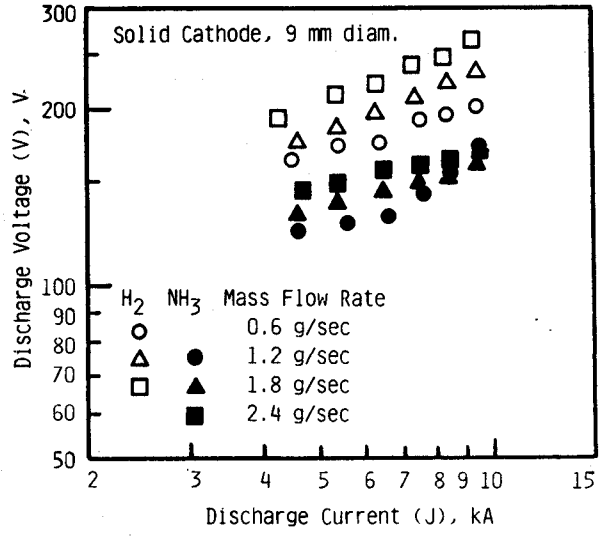

Fig. 13 Thrust efficiency vs ISP plot for a solid cathode.

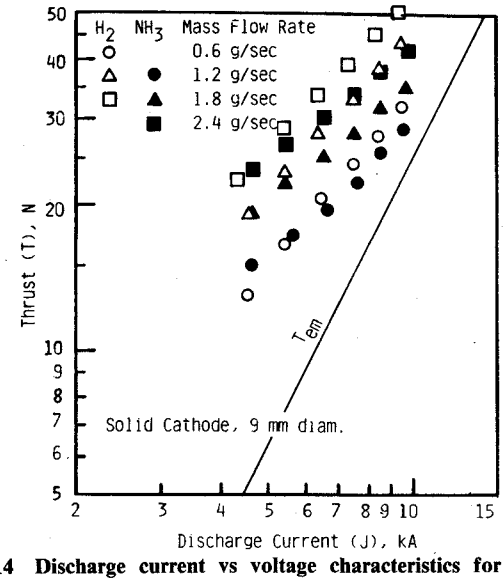

Fig. 14 Discharge current vs voltage characteristics for a solid cathode.

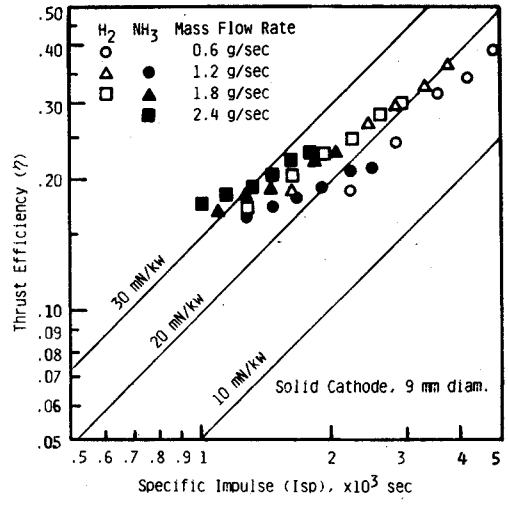

Fig. 15 Thrust vs current characteristics for a solid cathode.

terelectrode length seems ineffective. For ammonia propellant, results are confusing around the Isp of 2000 s because the constant mass flow is violated in this range by excessively high hollow cathode pressure.

Figure 12 shows the hollow cathode pressure variations for different interelectrode lengths. This result indicates that longer interelectrode length effectively leads to higher pressure by electrothermal heating in the arc column. The pressure reaches 3 atm for both hydrogen and ammonia. This fact suggests that the propellant is more effectively heated by elongating the arc column than by reducing the diameter. Elongation of the arc column would enhance the thermalization and probable energy transfer collision of high-speed electrons with heavy particles. However, these high hollow cathode pressures proved not always favorable to the fast-acting valves that regulate the mass flow rates at the maximum supply pressure of 5 atm. Therefore, strictly speaking, the data obtained at high hollow cathode pressures exceeding 2.6 atm might not be reliable for regulated mass flow rate. Such data were discarded from Figs. 9-11.

The cathodes and interelectrode insulator erosion rates are summarized in Table 2 for various hollow cathode diameters. Surprisingly, the cathode erosion rate is reduced in the smaller hollow cathode diameters where the intense arc spots are attached. This fact probably suggests that the cathode erosion process depends on the direction of pinch force induced in the hollow cathode interior. This will be discussed later, together with the effects of interelectrode length.

Effects of Interelectrode Length

Cathode and interelectrode insulator erosion rates for various interelectrode lengths are summarized in Table 3. As anticipated from the foregoing discussion, the insulator erosion rate is maximum for ammonia propellant in the case of the longest interelectrode length. This can be explained by the propellant shortage in the hollow cathode, which causes severe erosion for the longest insulator channel. As for the cathode erosion rates, they are reduced with increasing interelectrode length. This suggests that the cathode mass loss is inhibited by the rise in the interior pressure. Most of the eroded material from the cathode may be ionized and returned to the cathode surface again as the ion current.[9]

It is concluded from these results that elongation of the interelectrode effectively improves the hollow cathode performance during operation with hydrogen propellant but that the same conclusion cannot be applied to ammonia.

Table 4 Cathode and insulator erosion, $\mu g/C$, for solid cathode

	H_2	NH_3
Solid cathode	91.9	86.6
Insulator	−0.6[a]	7.1

[a] − = deposit.

Comparison with Solid Cathode Performance

The thrust efficiency is plotted against Isp in Fig. 13 for a solid 9-mm cathode. The results are almost identical to the best data obtained with solid cathode in our former experiments. The solid cathode configuration produced the thrust power ratio of about 25 mN/kW for hydrogen and 30 mN/kW for ammonia in the Isp range of 1000-2000 s. The hydrogen data are consistent with those obtained using a hollow cathode configuration, but the ammonia data exceed the hollow cathode results. The reason for this is simple; the solid cathode produces higher thrust with ammonia propellant than the hollow cathode at the same level of discharge voltage, as shown in Figs. 14 and 15. It must be pointed out that with the solid cathode, most of the arc current flows into the cathode tip for hydrogeneous propellants. Such current flow patterns never interrupt the propellant flow; however, the cathode erosion rate is more severe in the solid cathode than in the hollow cathode, as shown in Table 4.

In order to improve the thrust efficiency using a hollow cathode with ammonia propellant, higher propellant supply pressure to maintain the choked flow condition against the induced back force, together with the displacement of choking orifices from the fast-acting valves to the upstream hollow cathode passage, will be necessary.

Conclusions

Various hollow cathodes with different interior diameters and interelectrode lengths were tested to evaluate their performance in a quasisteady MPD thruster in the Isp range of 1000-2000 s. The following conclusions are drawn from the experimental results:

1) For hydrogen propellant, combining an appropriate hollow cathode diameter and interelectrode length, the hollow cathode MPD thruster produces the same level of thrust power ratio as the solid cathode. This is due to efficient electrothermal heating inside the arc column.

2) For ammonia propellant, the back pressure induced by both electromagnetic and electrothermal compression inside the hollow cathode made it difficult to regulate the predetermined mass flow rates. Consequently, the thrust performance was far inferior to that of a solid cathode. In order to overcome this problem, higher supply pressure, together with the displacement of choking orifices from the fast-acting valves to the hollow cathode interior, is necessary.

3) The cathode erosion rates were markedly reduced using hollow cathodes. The loss mechanism of cathode material was found to correlate strongly with both the electromagnetic pinch force and the electrothermally induced pressure in the hollow cathode internal passage.

References

[1]Esker, D.W., Kroutil, J.C., and Sedrick, A.V., "Cathode Studies of a Radiation Cooled MPD Arc Thruster," AIAA Paper 70-1083, 1970.

[2]Fradkin, D.W., Blackstock, A.W., Roehling, D.J., Stratton, T.F., Williams, M., and Liewer, K.W., "Experiments Using a 225-kW Hollow Cathode Lithium Vapor MPD Arcjet," *AIAA Journal,* Vol. 8, May 1970, pp. 886-894.

[3]Krishnan, M., Jahn, R.G., von Jaskowsky, W. F., and Clark, K.E., "Physical Processes in Hollow Cathodes," *AIAA Journal,* Vol. 15, Sept. 1977, pp. 1217-1223.

[4]Toki, K. and Kimura, I., *Progress in Astronautics and Aeronautics: Studies of Current Distribution on the Hollow Cathode of an MPD Arcjet,* Vol. 79, AIAA, New York, 1981, pp. 496-503.

[5]Kagaya, Y., Yokoi, Y., Tahara, H., and Yoshikawa, T., "Thrust Performance and Current Distribution in a Quasi-Steady MPD Arcjet," JSASS/AIAA/DGLR, Tokyo, IEPC 84-31, 1984.

[6]Burton, R.L., Clark, K.E., and Jahn, R.G., "Measured Performance of a Multimegawatt MPD Thruster," *Journal of Spacecraft and Rockets,* Vol. 20, May-June 1983, pp. 299-304.

[7]Jahn, R.G., *Physics of Electric Propulsion,* McGraw-Hill Book Co., New York, 1968.

[8]Uematsu, K., Mori, K., Kuninaka, H., and Kuriki, K., "Effect of Electrode Configuration on MPD Arcjet Performance," JSASS/AIAA/DGLR, Tokyo, IEPC 84-11, 1984.

[9]Kimblin, C.W., "Cathode Spot Erosion and Ionization Phenomena in the Transition from Vacuum to Atmospheric Pressure Arcs," *Journal of Applied Physics,* Vol. 45, Dec. 1974, pp. 5235-5244.